

## Comparison between chiral and meson-theoretic nucleon-nucleon potentials through $(p,p')$ reactions

F. Sammarruca and D. Alonso

*Physics Department, University of Idaho, Moscow, Idaho 83844*

E. J. Stephenson

*Indiana University Cyclotron Facility, Bloomington, Indiana 47408*

(Received 5 September 2001; published 25 March 2002)

We use proton-nucleus reaction data at intermediate energies to test the emerging new generation of chiral nucleon-nucleon ( $NN$ ) potentials. Predictions from a high-quality one-boson-exchange (OBE) force are used for comparison and evaluation. Both the chiral and OBE models fit  $NN$  phase shifts accurately, and the differences between the two forces for proton-induced reactions are small. A comparison to a chiral model with a less accurate  $NN$  description sets the scale for the ability of such models to work for nuclear reactions.

DOI: 10.1103/PhysRevC.65.047601

PACS number(s): 21.30.Fe, 25.40.Ep, 24.10.Cn, 24.70.+s

Chiral perturbation theory ( $\chi$ PT) offers a way to describe phenomena at nuclear physics energies that is consistent with the symmetries of the underlying theory of strong interactions (QCD). In this low-momentum regime, QCD itself is nonperturbative. In  $\chi$ PT, one expands chiral  $\pi N$  Lagrangians in powers of the relevant momenta or masses (e.g., pion mass), relative to the QCD scale at  $\Lambda_{\text{QCD}} \sim 1$  GeV. The nucleon-nucleon ( $NN$ ) force can then be derived from chiral Lagrangians by taking into account all pion-exchange diagrams which contribute to the  $NN$  interaction up through a given chiral order.  $NN$  potentials based on  $\chi$ PT are thus best suited for low-energy applications in nuclear structure or reactions. Only recently has a chiral  $NN$  potential become available through the work of Entem and Machleidt (EM) [1] that accurately reproduces  $NN$  phase shifts up to 325 MeV. In this paper, we present the first tests of this chiral potential using  $(p,p')$  reactions at 200 MeV.

Proton-nucleus elastic and inelastic scattering to selected transitions can be a “laboratory” for the evaluation of  $NN$  interactions to the extent that the reaction mechanism is dominated by a single  $NN$  scattering [2–4]. By choosing the quantum numbers of the transition (natural/unnatural parity, isoscalar/isovector) the  $(p,p')$  cross section and polarization observables (e.g., [5,6]) become selectively sensitive to specific amplitudes in the effective interaction in ways that complement  $NN$  scattering data. Here we will compare two recent  $\chi$ PT  $NN$  potentials [1,7] with the more conventional one-boson-exchange (OBE) CD-Bonn potential [8], using the  $(p,p')$  reaction to judge the suitability of the potential for nuclear reaction work. The two  $\chi$ PT potentials differ in the precision with which they reproduce  $NN$  phase shifts. This will calibrate for us the quality of agreement needed in  $\chi$ PT to describe well reactions such as proton-nucleus elastic and inelastic scattering. Previous studies using conventional potentials have demonstrated that good reproduction of  $(p,p')$  observables depends on a high-quality representation of the  $NN$  data [2].

The  $\chi$ PT expansion of EM [1] includes  $1\pi$  and  $2\pi$  diagrams from effective chiral Lagrangians, with relativistic corrections, through third order. The short-range repulsion is

described by including contact terms up through fourth order. To be suitable for iteration in a Lippmann-Schwinger equation, the potential is regularized through a set of cutoff masses. The resulting 46 model parameters were adjusted to match the  $NN$  phase shift solution from the Nijmegen group [9]. The agreement is excellent at energies below 325 MeV.

This  $\chi$ PT potential is based on a heavy-baryon expansion scheme where nucleon fields are represented by 2-component spinors. This makes a relativistic treatment of nucleons in nuclear matter [Dirac-Brueckner-Hatree-Fock (DBHF) approach] infeasible. Thus we will only include Brueckner-Hartree-Fock (BHF) medium effects when calculating density-dependent effective interactions. We start from a microscopic calculation of the nuclear force in nuclear matter where medium modifications arise from an effective nucleon mass (produced in a self-consistent calculation of nuclear matter saturation properties) and a spherically averaged Pauli blocking operator [10]. The resulting density-dependent  $G$  matrix is transformed into a Yukawa representation for use in distorted-wave impulse approximation (DWIA)  $(p,p')$  reaction calculations (see Appendix A of [2]).

The DWIA calculations are made with the programs LEA [11] for natural parity transitions and DWBA86 [12] for unnatural parity. The distortions are generated from the density-dependent effective interaction using the folding model. The form factors are chosen to conform to  $(e,e')$  measurements for the same transitions. The nuclear matter density is extracted from the charge density [13] by unfolding the form factor of the proton. Additional details may be found in Refs. [2,3].

The two largest amplitudes in the isoscalar effective interaction are the central and spin-orbit. These are best tested against natural parity transitions, including elastic scattering, in part because they exclude sensitivity to the tensor components. As a representative example, Fig. 1 (top panel) shows density-dependent calculations of the differential cross section and vector analyzing power for 200-MeV protons scattering elastically on  $^{40}\text{Ca}$ . There is good agreement between the chiral  $NN$  potential (solid curves) and the conventional OBE potential (long-dashed curves).

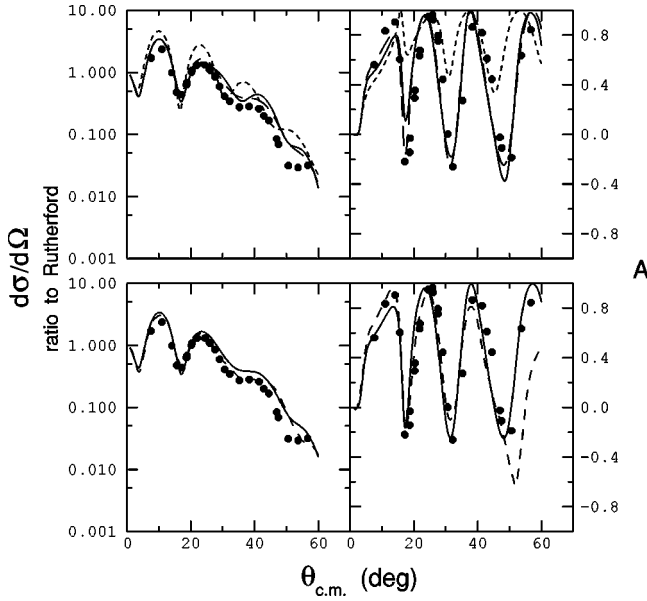


FIG. 1. Measurements for proton elastic scattering cross section (shown as the ratio to the Rutherford cross section) and analyzing power from Ref. [14]. The top panel shows calculations based on the chiral  $NN$  potential of Ref. [1] (solid curves) and the CD-Bonn potential of Ref. [8] (long-dashed curves). Both calculations contain BHF density dependence. The short-dashed curves are CD-Bonn potential calculations with no density dependence included. In the lower panel we compare the density-dependent predictions from the CD-Bonn model (solid line) to the predictions from Ref. [15] (dashed line).

Differences with the data [14] are a reasonable gauge of remaining theoretical uncertainties or approximations. Since the differences between the chiral and CD-Bonn curves are comparable to, or smaller than, the differences between either model and the data, we conclude that the EM chiral model is as satisfactory as the CD-Bonn model as the basis for reaction calculations, within the present context of reaction and scattering models. As a contrasting example, the short-dashed curve in the top panel of Fig. 1 uses the CD-Bonn interaction, but removes the BHF density dependence, leaving only the free  $NN$  interaction. This causes a large change, especially for the analyzing power, which is sensitive to the interference between central and spin-orbit amplitudes. The clear preference of the data for the medium-modified BHF calculation renders the free interaction by itself unsatisfactory. In the lower panel we compare our CD-Bonn calculation (solid line) with another modern distorted-wave model (dashed line) [15]. The latter differs mainly in the use of an exact finite-range treatment of knock-on exchange that, using the program DWBA91 [16], sums over all of the nucleons in  $^{40}\text{Ca}$  explicitly. This is in contrast to the zero-range approximation used for the exchange amplitude in the LEA program (the validity of which was also discussed in Ref. [2].) While the DWBA91 result agrees better with the cross section between  $20^\circ$  and  $40^\circ$  and the forward angle analyzing power, it has more difficulty with the larger-angle analyzing power. (Other differences exist between the calculations: Reference [15] uses the Paris  $NN$  interaction [17]

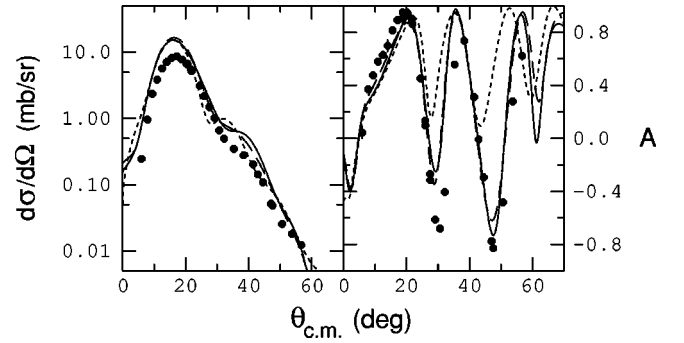


FIG. 2. Measurements for proton inelastic scattering cross section and analyzing power for the  $3^-$  state in  $^{40}\text{Ca}$  at 3.736 MeV from Ref. [14]. The curves are the same as in the top panel of Fig. 1.

and harmonic oscillator wave functions.) By our standard, neither calculation is clearly favored and both represent the current capability of distorted-wave impulse approximation calculations to describe elastic proton scattering.

With Fig. 2 we illustrate the same points using the  $3^-$  state at 3.736 MeV in  $^{40}\text{Ca}$ , with curves as in the top panel of Fig. 1 and the data from Ref. [14]. Again, the two BHF calculations are in good agreement with each other (while the free case is again unsatisfactory).

The largest parts of the isovector effective interaction are associated with the  $\sigma_1 \cdot \sigma_2$  and  $S_{12}(\hat{q})$  spin operators. These are best sampled in unnatural-parity transitions that are insensitive to the central terms, and “stretched” transitions with  $J = j_{\text{part}} + j_{\text{hole}}$  offer the advantages of a simple structure that is easily constrained by  $(e, e')$  data and surface peaking in the form factor that minimizes medium effects.

Figure 3 presents the chiral and CD-Bonn calculations (solid and dashed curves, respectively) for the  $4^-$ ,  $T=1$  transition in  $^{16}\text{O}$  to the state at 18.98 MeV. BHF density dependence is included, and isospin mixing follows the prescription of Carr *et al.* [18]. The measurements are taken from Refs. [19,20]. The agreement between the two potentials and with the measurements is excellent. In particular,

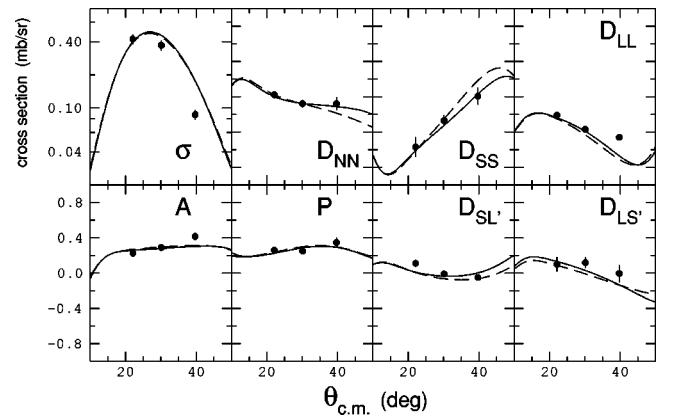


FIG. 3. Measurements of the cross section and polarization observables for the transition to the  $4^-$ ,  $T=1$  state at 18.98 MeV in  $^{16}\text{O}$  from Refs. [19,20]. The solid (dashed) curves are based on the chiral potential of Ref. [1] (the CD-Bonn potential of Ref. [8]).

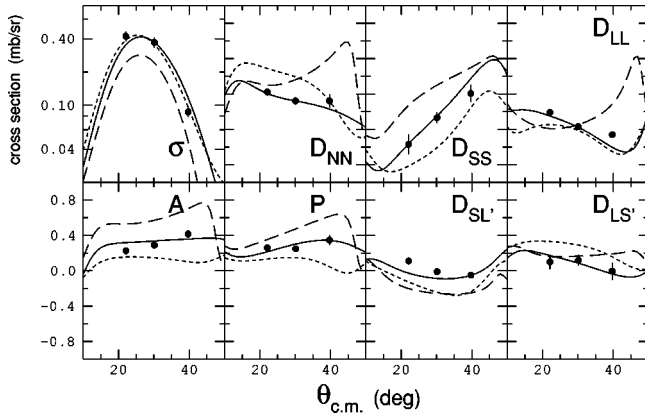


FIG. 4. The measurements are described in Fig. 3. The solid curves are based on the chiral potential of Ref. [1]. The long- and short-dashed curves are based on the NLO and NNLO potentials of Ref. [7].

the good agreement with the diagonal polarization transfer coefficients  $D_{ii}$  demonstrates that the relative sizes of the spin-orbit and three tensor amplitudes are well reproduced for both the EM chiral and CD-Bonn potentials [5,6]. Interestingly, the chiral potential shows better agreement with the data for  $D_{NN}$  and  $D_{SS}$  than does the original CD-Bonn potential. This improvement comes from a small reduction in the spin-longitudinal amplitude (associated with the  $\sigma_{1q}\sigma_{2q}$  tensor operator).

Since we conclude that the EM chiral model reproduces the large  $NN$  amplitudes as well as the best of the OBE models, it is appropriate to ask whether agreement of a lesser quality could also be satisfactory for  $(p,p')$  reaction work. In EM [1], the reproduction of the  $NN$  phase shifts up to 300 MeV was compared to the predictions from the second-order [or next-to-leading order (NLO)] and the third-order [or next-to-next-to-leading order (NNLO)] potentials of Ref. [7]. The second-order interaction from that work has been used recently as the basis for Faddeev calculations of three-body observables [21]. Some success was found for energies near and below 10 MeV. However, at 200 MeV the phase shift predictions diverge [1]. To illustrate the effect on  $(p,p')$  reactions, in Fig. 4 we again show the polarization measurements for the  $4^-$ ,  $T=1$  state in  $^{16}\text{O}$ . The solid curves are based on the EM chiral model. Since medium effects are small here, these are free-space predictions (compare with the solid curves in Fig. 3). The long-dashed and short-dashed curves in Fig. 4 show the NLO and NNLO interactions of Ref. [7], respectively. The NNLO contains pion-exchange

contributions to the same order as in EM. The main difference is that EM have included contact terms to fourth order and increased the number of momentum cutoff parameters. While this increases the number of free parameters to be determined from the  $NN$  phase shifts, it also provides the flexibility necessary for an accurate fit at higher energies. The NLO and NNLO curves shown in Fig. 4 both differ dramatically from the measurements and even at NNLO do not appear to be converging except for the cross section. These differences exceed by an order of magnitude those shown in Fig. 3. This sets a scale for how much better the phase shift reproduction must be before it makes sense to compare these chiral potential predictions with nuclear reaction measurements at the level of conventional models. The chiral potential of EM meets this standard.

The  $\chi$ PT model of EM gives rise to a number of solutions that differ in some of their short-range characteristics. This is illustrated by excellent agreement with the long-range properties of the deuteron (binding energy, quadrupole moment, asymptotic  $S$  and  $D$  states, and the mean radius) while allowing the  $D$ -state probability to vary by a factor of 2. These solutions provide comparable fits to  $NN$  phase shifts. Thus the handling of the short-range part via contact terms brings about a larger degree of flexibility as compared to the usual meson-exchange picture (where, for instance, the strength of the tensor force as measured from the deuteron  $D$ -state probability is much more tightly constrained). Because of the restrictions imposed by the  $\chi$ PT expansion on the typical momenta involved in  $NN$  scattering or a nuclear reaction, it may not be possible to explore and control these ambiguities by going to higher energies. Instead, we may need to examine other nuclear reactions in situations that emphasize the upper end of the allowed momentum range, such as one finds in large-angle scattering or where the only contributing amplitudes come from nucleon exchange. Further investigation of the  $\chi$ PT predictive power will be pursued in future work.

The test calculations shown here demonstrate that  $\chi$ PT models of the  $NN$  interaction can be made with sufficient accuracy to be used in calculations of nucleon-induced reactions on nuclei, at least up to 200 MeV. For this, a high-precision reproduction of the  $NN$  scattering phase shifts is an essential first requirement. This means that models intended for wide application must contain a sufficient amount of flexibility to make such a high-precision reproduction possible.

The authors acknowledge financial support from the U.S. Department of Energy under Grant No. DE-FG03-00ER41148 (F.S. and D.A.) and from the National Science Foundation under Grant No. NSF-PHY-9602872 (E.S.).

- [1] D.R. Entem and R. Machleidt, Phys. Lett. B **524**, 93 (2002).  
 [2] F. Sammarruca, E.J. Stephenson, and K. Jiang, Phys. Rev. C **60**, 064610 (1999).  
 [3] F. Sammarruca, E.J. Stephenson, K. Jiang, J. Liu, C. Olmer, A.K. Opper, and S.W. Wissink, Phys. Rev. C **61**, 014309 (2000).  
 [4] F. Sammarruca and E.J. Stephenson, Phys. Rev. C **64**, 034006

- (2001).  
 [5] J.M. Moss, Phys. Rev. C **26**, 727 (1982).  
 [6] E. Bleszynski, M. Bleszynski, and C.A. Whitten, Jr., Phys. Rev. C **26**, 2063 (1982).  
 [7] E. Epelbaum, W. Glöckle, and Ulf-G. Meißner, Nucl. Phys. **A637**, 107 (1998); **A671**, 295 (2000).  
 [8] R. Machleidt, Phys. Rev. C **63**, 024001 (2001).

- [9] V.G.J. Stoks *et al.*, Phys. Rev. C **48**, 792 (1993).
- [10] M.I. Haftel and F. Tabakin, Nucl. Phys. **A158**, 1 (1970).
- [11] James J. Kelly, program manual for LEA, 1995.
- [12] R. Schaeffer and J. Raynal, program DWBA70; S. Austin, W. G. Love, J. R. Comfort, and C. Olmer, extended version DWBA86 (unpublished).
- [13] H. de Vries, C.W. de Jager, and C de Vries, At. Data Nucl. Data Tables **36**, 495 (1987).
- [14] H. Seifert *et al.*, Phys. Rev. C **47**, 1615 (1993).
- [15] P.J. Dortmans, K. Amos, and S. Karataglidis, J. Phys. G **23**, 183 (1997); K. Amos, P.J. Dortmans, H.V. von Geramb, S. Karataglidis, and J. Raynal, Adv. Nucl. Phys. **25**, 275 (2000).
- [16] J. Raynal, computer code DWBA, Report No. NEA 1209/02.
- [17] M. Lacombe, B. Loiseau, J.M. Richard, R. Vinh Mau, J. Côté, P. Pirès, and R. de Tourriel, Phys. Rev. C **21**, 861 (1980); as developed in L. Rikus, K. Nakano, and H.V. von Geramb, Nucl. Phys. **A414**, 413 (1984).
- [18] J.A. Carr, F. Petrovich, D. Halderson, D.B. Holtkamp, and W.B. Cottingham, Phys. Rev. C **27**, 1636 (1983).
- [19] A.K. Opper, S.W. Wissink, A.D. Bacher, J. Lisantti, C. Olmer, R. Sawafta, E.J. Stephenson, and S.P. Wells, Phys. Rev. C **63**, 034614 (2001).
- [20] C. Olmer, in *Antinucleon- and Nucleon-Nucleus Interactions*, edited by G. E. Walker *et al.* (Plenum, New York, 1985), p. 261.
- [21] E. Epelbaum, H. Kamada, A. Nogga, H. Witała, W. Glöckle, and Ulf-G. Meißner, Phys. Rev. Lett. **86**, 4787 (2001).